https://dx.doi.org/10.4314/IJS.v28i1.9



# SYNTHESIS, CHARACTERISATION AND ANTIMICROBIAL ACTIVITY OF METAL(II) COMPLEXES OF ALKYLATED MERCAPTOBENZIMIDAZOLE DERIVATIVES

**Sam, E. and Olalekan, T. E.***

Department of Chemistry, Faculty of Science, University of Ibadan, Ibadan, Nigeria.

*Corresponding author: topeolalekan11@yahoo.com

(Received: 27th February, 2026; Accepted: 28th March, 2026

Iron(II), cobalt(II), nickel(II), and copper(II) complexes of alkylated derivatives of 2-mercapto-5-nitrobenzimidazole (**5NMT**) were prepared via reflux reactions with 1,2-dibromoethane and the corresponding metal(II) salts in alkaline conditions. Characterisation of the compounds was carried out using CHNS elemental analysis, infrared and ultraviolet-visible spectroscopy, and magnetic susceptibility measurements. Their antimicrobial activity was evaluated against four bacterial and two fungal strains using the agar well diffusion method. In comparison, the infrared spectra of **5NMT** and the metal complexes presented shifts in the N–H and C–N stretching vibrations, consistent with coordination through the benzimidazole nitrogen atom. The magnetic moment values, electronic spectral and elemental analytical data were collectively employed to propose the probable coordination geometries of the complexes. From the synthesised compounds, the Cu(II) complex exhibited the highest antibacterial activity, with inhibition zones between 10 and 20 mm. Both *Aspergillus niger* and *Candida albicans* were susceptible to all the metal complexes, suggesting that the complexes warrant further screening against additional fungal strains to better assess their antifungal potential.

**Keywords:** 2-Mercapto-5-nitrobenzimidazole, Coordination complexes, *S*-alkylation, Characterisation, Antifungal activity.

## INTRODUCTION

Benzimidazoles are heterocyclic compounds that have shown relevance in various applications, and particularly in medicinal chemistry (Baron *et al*., 2022; Champa *et al*., 2023; Rep *et al*., 2022). 2-Substituted benzimidazole derivatives were evaluated for biological applications, and were found to exhibit anticancer (Theodore *et al*., 2023; Aragón-Muriel *et al*., 2021), antibacterial and antifungal (Arya *et al*., 2025; Neshat *et al*., 2023; Desai *et al*., 2024), antioxidant (Bektaş *et al*., 2020), and antiplasmodial (Purwono *et al*., 2021) activities. An important derivative of benzimidazole is 2-mercaptobenzimidazole (or 2-benzimidazolethiol), which has been used to generate many organic products by substituting the thiol proton, and by derivatizing the nitrogen heteroatom. Some 2-mercaptobenzimidazole-derived compounds have demonstrated antimicrobial and anticancer (Aroua e*t al*., 2023; Rizvi *et al*., 2020; Al-Mahdawi *et al*., 2025), acetylcholinesterase inhibitory (Begum *et al*., 2022), and anti-browning/tyrosinase inhibitory (Lee *et al*., 2023) activities. Their applications in corrosion inhibition (Jakeria *et al*., 2022; Ji *et al*., 2021; Khormali and Ahmadi, 2023) and in dye removal (Elwakeel *et al*., 2021) have been reported. The antidiabetic (Patle *et al*., 2023), antitubercular (Popovici *et al*., 2021; Cheptea *et al*., 2022), anticancer, acetylcholinesterase and butyrylcholinesterase inhibitory properties (Alpan *et al*., 2017; Sarıkaya *et al*., 2018; El-Gohary *et al*., 2017) of 2-mercapto-5-nitrobenzimidazole derivatives have been investigated. Synthesis of 2-benzimidazolethiol derivatives has been carried out mainly in alkaline media, using various reagents. *S*-alkylation or -arylation was achieved in the presence of NaOH and appropriate alkylhalide (Rodríguez *et al*., 2021; Bespalov *et al*., 2015), trialkylphosphite and phosphorus oxychloride (El-Kihel *et al*., 2016), potassium carbonate (Champa *et al*., 2023; Nuha et al., 2021), and cesium carbonate (Subimol *et al*., 2015). Aminomethylation was achieved with dicyclohexyl-carbodiimide and 4-dimethylaminopyridine (DCC/DMAP) by Rodríguez *et al* (2021), while Bespalov *et al* (2015) used morpholine, and potassium carbonate and alkyl ester halide were also successfully used by Bektaş *et al* (2020). The disulfide derivatives were obtained by Molou and his co-researchers (2022) by reacting the parent thiols with diiodomethane in glacial acetic acid. Iodine, sodium bicarbonate and concentrated hydrochloric acid yielded the desired disulfide products from the parent thiols (Wei *et al*., 2021), while rosolic acid (Singh and Baruah, 2008), and electrochemical dehydrogenative coupling Zhang *et al.* (2022) were used to derive similar products. In view of important biological activities associated with

many benzimidazole-based molecules, interested researchers continue to synthesise and investigate new derivatives for improved medicinal applications. Although broader benzimidazolethiol libraries have been synthesised and tested for antifungal and anti-inflammatory activity, specific nitro-benzimidazolethiols remain underexplored. In this study, new metal complexes of alkylated derivatives of **5NMT** were synthesised, and characterised by CHNS elemental, infrared and UV spectral analyses and room-temperature magnetic susceptibility measurements. The antimicrobial properties of the metal compounds were investigated against six microbial pathogens/strains.

## MATERIALS AND METHODS

### General

The reagents and solvents were of analytical grade and were used as supplied. Melting points were determined on Gallenkamp melting point apparatus. The purity of the synthesised compounds was checked by TLC using Silica Gel as stationary phase and ethyl acetate-hexane (1:3) as eluent, the spots were visually detected in an iodine chamber. Elemental analyses (CHNS) were determined on Elementar Analysen systeme varioMICRO V1.6.2 GmbH. The infrared spectra were obtained as KBr discs on a Perkin-Elmer FTIR spectrophotometer in the range 4000–400 $cm^{-1}$. UV/Visible spectra were obtained in DMF solvent on Labomed UV-Vis Spectrophotometer in the ranges 190-400 and 400-900 nm, respectively. Magnetic susceptibility measurements were recorded on a Sherwood magnetic susceptibility balance MSB Mark 1 and diamagnetic corrections were calculated using Pascal's constants.

### Synthesis Procedure

The metal complexes of the alkylated derivatives of 5-nitrobenzimidazolethiol were generally prepared using a template synthesis method. 2-Mercapto-5-nitrobenzimidazole (**5NMT**) (0.2796 g, 1.432 mmol) in 10 mL ethanol was stirred on a hot plate, while an ethanol solution containing sodium hydroxide (0.1146 g, 2.864 mmol), 1, 2-dibromoethane (0.1 mL, 1.432 mmol) were added sequentially, dropwise. After refluxing the mixture for 3 h, the solution of metal salt (0.716 mmol) in 3 mL ethanol was added, and the mixture was further heated to reflux for 1 h. Each precipitate was obtained by filtration, washed with ethanol and dried in air. The purity of the derived products was ascertained by a single spot shown by thin layer chromatography procedure.

**[M1].EtOH:** $FeSO_4.7H_2O$ (0.1991 g, 0.716 mmol) was used. Yellow solid; yield, 0.2241 g, 52%; M.pt 178-180 °C. Anal. Calc. for $C_{36}H_{36}Fe_2N_{12}O_{18}S_6$ (Mr = 1228.80): C 35.19, H 2.95, N 13.68, S 15.65%. Found: C 35.33, H 2.65, N 14.86, S 14.90%.

**[M2].10$H_2O$:** $CoCl_2.6H_2O$ (0.1704 g, 0.716 mmol) was used. Green solid; yield, 0.1470 g, 39.3%; Dec 278 °C. Anal. Calc. for $C_{18}H_{36}Br_2Cl_4Co_2N_6O_{14}S_2$ (Mr = 1044.11): C 20.71, H 3.48, N 8.05, S 6.14%. Found: C 19.77, H 2.79, N 8.58, S 6.31%.

**[M3].EtOH:** $NiCl_2.6H_2O$ (0.1702 g, 0.716 mmol) was used. Yellow solid; yield, 0.1535 g, 42.5%; M.pt 170-172 °C. Anal. Calc. for $C_{34}H_{30}N_{12}NiO_9S_4$ (Mr = 1008.52): C 40.49, H 3.00, N 16.67, S 12.72%. Found: C 41.62, H 3.01, N 17.19, S 13.15 %.

**[M4].$H_2O$:** $CuCl_2.2H_2O$ (0.1220 g, 0.716 mmol) was used. Brown solid; yield, 0.2522 g, 61.9%; M.pt 216-218 °C. Anal Calc. for $C_{16}H_{14}Cl_2CuN_6O_5S_2$ (Mr = 568.90): C 33.78, H 2.48, N 14.77, S 11.27%. Found: C 34.58, H 2.15, N 14.21, S 10.13%.

### Antimicrobial Screening Assay

The *in vitro* antimicrobial properties of complexes **M1–M4** were investigated against four bacterial strains (*Staphylococcus aureus*, *Bacillus subtilis*, *Pseudomonas aeruginosa*, and *Escherichia coli*) as well as two fungal strains (*Aspergillus niger* and *Candida albicans*), employing the agar well diffusion technique. Gentamycin (10 μg/mL) and ketoconazole (1%) were used as reference drugs for antibacterial and antifungal evaluations, respectively, whereas dimethylformamide (DMF) served as the negative control. Microbial inocula were prepared by culturing each test organism on agar at 37 °C for 18–24 h and adjusting the turbidity to match the 0.5 McFarland standard. A loopful of each stock culture was transferred into 5 mL of sterile nutrient broth and incubated under the same conditions for 18–24 h. Subsequently, 0.1 mL of the overnight culture was diluted with 9.9 mL of sterile distilled water (1:100 dilution). An aliquot (0.2 mL) of this suspension was aseptically mixed with sterile molten nutrient agar and poured into sterile Petri dishes to solidify. Wells of 8 mm diameter were created in the solidified agar using a

sterile cork borer, and 0.20 mL (80 μg) of each test compound was introduced into the respective wells. The experiment was performed in replicate. The plates were allowed to stand at room temperature for 1 h to facilitate pre-diffusion before incubation at 37 °C for 18–24 h. The antimicrobial activity was assessed by measuring the diameters of inhibition zones (in mm), as summarized in Table 3.

## RESULTS AND DISCUSSION

The complexes were soluble in methanol, acetone, DMF and DMSO, and had melting points between 170 and 218 °C, while the cobalt(II) complex decomposed at 218 °C**.** The CHNS elemental analysis was found to be in good agreement with the calculated values for each proposed metal complex.

### Infrared Spectra

The infrared spectra of the complexes and the benzimidazole precursor (**5NMT**), recorded in **Table 1**, were obtained to indicate the binding sites. The broad bands found in the spectra of the complexes, **M1**–**M4**, in the range 3363–3305 $cm^{-1}$ and 750 $cm^{-1}$ showed the presence of O-H bands in $H_2O$ or $C_2H_5OH$ environment (Coates, 2000). The N–H stretching frequency appeared as a strong broad band at 3143 $cm^{-1}$ in **5NMT** (Champa *et al*., 2023), while it was shifted to lower wavenumbers in the range 3112 – 3101 $cm^{-1}$ in the metal complexes. Though a slight shift was recorded for $\nu$(C=N) found at approximately 1620 $cm^{-1}$ in the compounds, a corresponding increase in $\nu$(C–N) from 1244 $cm^{-1}$ (**5NMT**) to 1263–1258 $cm^{-1}$ in the complexes also demonstrated the binding through the benzimidazole nitrogen atom. Thioalkylation of the benzimidazolethiol group was shown by the disappearance of the weak and broad S–H band in the complexes, which has been observed at 2433 $cm^{-1}$ in **5NMT** (Coates, 2000). This was also supported by the appearance of new weak bands in the spectra of **[M1]**–**[M4]**. These bands in the ranges 1463–1441 $cm^{-1}$ and 660–657 $cm^{-1}$, were assigned to δ(-$CH_2$-) and $\nu$(-$CH_2$-S), respectively (Coates, 2000; El Ashry, *et al*., 2016). The non-coordination of the sulphur atom was suggested by the $\nu$(C–S) at 687 $cm^{-1}$, which was only slightly shifted in the complexes to the range of 689–698 $cm^{-1}$. The strong bands at 1592 and/or 1540 $cm^{-1}$ were assigned to $\nu$(C=C), while the asymmetric and symmetric stretching frequencies of $NO_2$ appeared around 1520 and 1350 $cm^{-1}$ in the compounds. The complex **[M2]** showed two distinct medium intense band at 1060 and a weak band at 672 $cm^{-1}$, assigned to the asymmetric and symmetric stretches of the sulphato ion. The absence of a band above 1200 $cm^{-1}$, suggested the coordination of the sulphato ion in a bridging mode. Similarly, the medium and broad band at 600 $cm^{-1}$, was designated to $\nu$(C–Br) in **[M2]** (Coates, 2000). These bands were absent in the spectra of other complexes. The new medium to weak bands in the range 477–436 $cm^{-1}$, were assigned to M–N stretching frequencies in **[M1]**–**[M4]**, while the band at 500 $cm^{-1}$ was designated to $\nu$(Fe–O).

**Table 1:** The infrared stretching and bend frequencies of the compounds in $cm^{-1}$

| Compounds | 5NMT | [M1] | [M2] | [M3] | [M4] |
|---|---|---|---|---|---|
| O–H | ---- | 3358, 752 | 3363, 753 | 3305, 752 | 3351, 753 |
| N–H | 3143 | 3103 | 3107 | 3112 | 3101 |
| S–H | 2433 | ---- | ---- | ---- | ---- |
| C=N | 1625 | 1620 | 1622 | 1621 | 1620 |
| C=C | 1534 | 1592, 1543 | 1594 | 1594 | 1595 |
| $NO_2$ | 1513, 1355 | 1520, 1347 | 1522, 1346 | 1522, 1347 | 1523, 1345 |
| $CH_2$ | ---- | 1460 | 1455 | 1441 | 1463 |
| C–N | 1244 | 1258 | 1263 | 1259 | 1258 |
| $SO_4^{2-}$ | ---- | 1060, 672 | ---- | ---- | ---- |
| C–S | 687 | 689 | 698 | 690 | 693 |
| $CH_2$–S | ---- | 657 | 660 | 657 | 660 |
| C–Br | ---- | ---- | 600 | ---- | ---- |
| M–N | ---- | 521, 440 | 436 | 442 | 477 |

### Electronic Spectra and Magnetic Moments

The electronic spectra of the compounds are recorded in Table 2. The intense UV absorptions in the ranges 281–295 nm and 317–327 nm were respectively assigned to $\pi \rightarrow \pi^*$ and $n \rightarrow \pi^*$ transitions. The single transition expected for

Fe(II) complexes in either octahedral ($^5T_{2g} \rightarrow {}^5E_g$, 900–1000 nm) or tetrahedral geometry ($^5E \rightarrow {}^5T_2$, ~2500 nm) was not observed (Greenwood and Earnshaw, 1998(a)). However, an intense charge transition was observed at 416 nm. For high-spin octahedral Fe(II) complexes, a magnetic moment of 5.2–5.4 BM is expected due to orbital contribution or stereochemical distortions, while the tetrahedral complexes were reported to lie in the range 5.0-5.4 BM (Greenwood and Earnshaw, 1989(a)). The observed magnetic moment for **[M1]** was 5.1 BM, which was suitable for a tetrahedral configuration. In either the tetrahedral or octahedral Co(II) geometry, three spin-allowed transitions are expected, where the tetrahedral spectra usually consist of a broad, intense band in the visible region with a weaker one in the infrared (Greenwood and Earnshaw, 1998(b)). The reported complex exhibited a broad band at 635 nm, assigned to $^4A_2 \rightarrow {}^4T_1$ (P) ($\nu_3$) transition in the tetrahedral symmetry, while the other two transitions ($\nu_1$ and $\nu_3$) were not observed as they usually appear in the infrared region 3000–8000 $cm^{-1}$ (Greenwood and Earnshaw, 1998(b)). An intense charge transfer transition appeared in the Co(II) complex at 425 nm. The magnetic moment of 4.5 BM derived for **[M2]** suggested a tetrahedral structure since it lies within the range 4.4-4.8 BM, and was outside that for octahedral complexes (4.8-5.2 BM) (Greenwood and Earnshaw, 1998(b)). Three transitions could be seen in the spectra of octahedral and tetrahedral Ni(II), where those arising from the latter geometry are usually more intense. On the other hand, the spectra of square-planar Ni(II) complexes are usually characterised by a fairly strong band between 450 and 600 nm, as well as another band near the ultraviolet region. The reported Ni(II) complex **[M3]** showed a strong band at 432 nm, and a charge transfer transition at 416 nm. The magnetic moments of tetrahedral and octahedral compounds have been reported in the ranges 3.2-4.1 BM and 2.9-3.3 BM, respectively. (Greenwood and Earnshaw, 1998(c)). The observed magnetic moment of 0.8 BM suggested a square planar geometry for **[M3]**, and the electronic transition at 432 nm could be assigned to $^1A_1g \rightarrow {}^1B_1g$ transition. The copper(II) complex **[M4]** exhibited a visible band at 414 nm, assigned to the square planar $^2B_{1g} \rightarrow {}^2A_{1g}$ transition. The intense charge transfer transition was observed at 405 nm.

**Table 2:** UV-Vis bands (λ, nm) and magnetic moments of the synthesised compounds

| Compounds | $\pi \rightarrow \pi^*$ | $n \rightarrow \pi^*$ | LM | d → d | $\mu_{eff}$ ($\mu_B$) | |
|---|---|---|---|---|---|---|
| **[M1]** | 282, 294 | 317 | | 416 | ---- | 5.1 |
| **[M2]** | 281, 295 | 327 | | 425 | 635 | 4.5 |
| **[M3]** | 291 | 322 | | 416 | 432 | 0.8 |
| **[M4]** | 294 | 322 | | 405 | 414 | 1.4 |

LM = ligand to metal charge transfer

### *In vitro* Antimicrobial Activity: Inhibition Zone Diameters

The inhibition zones (mm) of the antimicrobial assay of the complexes **[M1]**–**[M4]** are presented in Table 3. The complex **[M1]** exhibited no antibacterial activity but showed antifungal effects against *A. niger* (16 mm) and *C. albicans* (12 mm), indicating preferential activity toward fungal strains. **[M2]** demonstrated limited antibacterial activity, showing inhibition only against *B. subtilis* (12 mm), while retaining moderate antifungal activity against *A. niger* (18 mm) and *C. albicans* (12 mm). This suggested a slight enhancement in activity relative to **[M1]**. The Ni(II) complex, **[M3]**, displayed broader antimicrobial activity, inhibiting *S. aureus* (10 mm), *P. aeruginosa* (12 mm), and *E. coli* (12 mm), in addition to pronounced antifungal activity against *A. niger* (20 mm) and *C. albicans* (16 mm). The expanded spectrum may indicate improved cell membrane permeability or enhanced interaction with microbial targets. **[M4]** exhibited the most significant overall activity among the tested compounds. It showed antibacterial effects against all four bacterial strains, with inhibition zones of 10 mm (*S. aureus*), 16 mm (*B. subtilis*), 10 mm (*P. aeruginosa*), and 12 mm (*E. coli*). Notably, it demonstrated strong antifungal activity against both *A. niger* and *C. albicans* (20 mm each). The improved activity of this Cu(II) complex may be attributed to structural modifications or possible metal coordination effects, which can enhance lipophilicity and facilitate penetration through microbial cell membranes. The standard antibacterial (gentamicin) and antifungal (ketoconazole) exhibited superior activities at 22–24 mm and 25–

27 mm, respectively. Although the synthesised compounds demonstrated lower activity compared to the standards, the Ni(II) and Cu(II) complexes displayed moderate broad-spectrum activity, particularly against fungal strains.

**Table 3:** The antimicrobial assay as diameters of inhibition zones (mm)

| Compounds | *S. aureus* | *B. subtilis* | *P. aeruginosa* | *E. coli* | *A. niger* | *C. albicans* |
|---|---|---|---|---|---|---|
| **[M1]** | --- | --- | --- | --- | 16 | 12 |
| **[M2]** | --- | 12 | --- | --- | 18 | 12 |
| **[M3]** | 10 | --- | 12 | 12 | 20 | 16 |
| **[M4]** | 10 | 16 | 10 | 12 | 20 | 20 |
| DMF | --- | --- | --- | --- | --- | --- |
| Gentamicin | 22 | 24 | 22 | 22 | --- | --- |
| Ketoconazole | --- | --- | --- | --- | 25 | 27 |

## CONCLUSION

In this study, iron(II), cobalt(II), nickel(II), and copper(II) complexes of alkylated derivatives of 2-mercapto-5-nitrobenzimidazole (5NMT) were successfully synthesised under alkaline conditions and characterised. The CHNS elemental analyses corroborated the proposed stoichiometries, while infrared spectral data confirmed *S*-alkylation of the parent thiol and coordination predominantly through the benzimidazole nitrogen atom. The observed shifts in the N–H and C–N stretching vibrations, together with the appearance of new M–N bands in the far-IR region, provided strong evidence for metal–ligand bond formation. Electronic spectral features and magnetic susceptibility measurements further supported the proposed coordination geometries for the respective metal centres. Hence, the metal complexes are proposed to have the structures shown in **Figure 1**.

The antimicrobial screening revealed the Cu(II) complex exhibiting the most pronounced antibacterial effect against the tested strains. Notably, all synthesised complexes demonstrated appreciable antifungal activity against *Aspergillus niger* and *Candida albicans*, indicating that metal coordination plays a significant role in modulating bioactivity, possibly through increased lipophilicity and improved cellular permeability. The research highlighted the potential of the development of alkylated **5NMT** metal complexes as metal-based antimicrobial agents, at a time of increasing resistance to conventional drugs. Further studies involving expanded microbial panels, minimum inhibitory concentration (MIC) determinations, and mechanistic investigations are recommended to fully elucidate their therapeutic potential and structure–activity relationships.

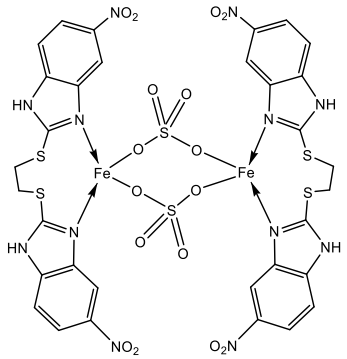


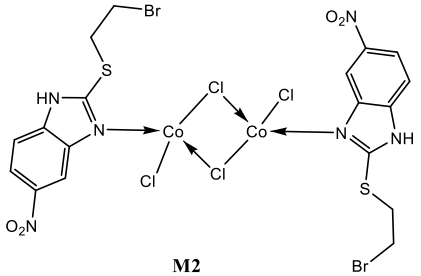

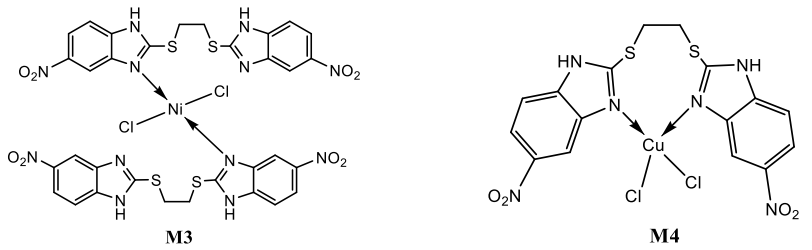


**Figure 1:** Proposed structures of the synthesised compounds

**ACKNOWLEDGEMENTS**

The authors thank Professor Norah Barba-Behrens, Departamento de Química Inorgánica y Nuclear, Universidad Nacional Autónoma de México, Coyoacan, Mexico, for supply of 5-nitrobenzimidazolethiol; Sunday Makinde, Department of Pharmaceutical Chemistry, Faculty of Pharmacy, University of Ibadan, for carrying out the antimicrobial assay.

**CONFLICTS OF INTEREST**

The authors declare there are no potential conflicts of interest.

**FUNDING**

This work was not funded by any institution, organization or entity.

**AUTHORS' CONTRIBUTION**

**T.E.O.:** Conceptualization, formal analysis, project administration, validation, writing – original draft preparation, review & editing. **E.S.:** Investigation, validation, formal analysis, writing – original draft preparation.

**REFERENCES**

Al-Mahdawi, A.S, Al-Obaidi, N.S, Ahmad, A.A, Jumaa, T.A, Abas, Z.A. and Mahdi, H.S., 2024. Synthesis, characterization and evaluation of biological activity of some 2-mercaptobenzimidazole complexes. *Results in Chemistry,* 13: 101893. doi: 10.1016/j.rechem.2024.101893

Alpan, A.S, Sarıkaya, G, Çoban, G, Parlar, S, Armagan, G. and Alptüzün, V., 2017. Mannich-Benzimidazole derivatives as antioxidant and anticholinesterase inhibitors: synthesis, biological evaluations, and molecular docking study. *Archiv der Pharmazie*, 350(7): e1600351, 5 pages. doi: 10.1002/ardp.201600351

Aragón-Muriel, A, Liscano, Y, Upegui, Y, Robledo, S.M, Ramírez-Apan, M.T, Morales-Morales, D, Oñate-Garzón, J. and Polo-Cerón, D., 2021. In vitro evaluation of the potential pharmacological activity and molecular targets of new benzimidazole-based Schiff base metal complexes. *Antibiotics,* 10(6): 728. doi: 10.3390/antibiotics10060728

Aroua, L.M, Alhag, S.K, Al-Shuraym, L.A, Messaoudi, S, Mahyoub, J.A, Alfaifi, M.Y. and Al-Otaibi, W.M., 2023. Synthesis and characterization of different complexes derived from Schiff base and evaluation as a potential anticancer, antimicrobial, and insecticide agent. *Saudi Journal of Biological Sciences***,** 30: 103598, 12 pages. doi: 10.1016/j.sjbs.2023.103598

Arya, C.G, Kumari, J, Kishan, J, Goswami, K, Sriram, D, Salim, S.A, Pakhira, P, Busi, S, Alharbi, M, Chandrakanth, M, Pasupuleti, M. and Banothu, J., 2025. 2-Substituted and 1,2-disubstituted benzimidazole derivatives: synthesis and identification of potential antibacterial agents. *Journal of Molecular Structure*, 1333: 141693. doi: 10.1016/j.molstruc.2025.141693

Baron, A, Sann, C.L. and Mann, J., 2022. Symmetric bis-benzimidazoles as DNA minor groove-binding agents with anti-tumour and antibacterial activity, and the evolution of the drug ridinilazole for the treatment of *Clostridium difficile* infections. *Bioorganic & Medicinal Chemistry*, 58: 116656. doi: 10.1016/j.bmc.2022.116656

Begum, F, Rehman, N.U, Khan, A, Iqbal, S, Paracha, R.Z, Uddin, J, Al-Harrasi, A. and Lodhi, M.A., 2022. 2-Mercaptobenzimidazole clubbed hydrazone for Alzheimer's therapy: *In vitro*, kinetic, *in silico*, and *in vivo* potentials. *Frontiers in pharmacology*, 13: 946134, 14 pages.
doi: 10.3389/fphar.2022.946134

Bektaş, H, Sökmen, B.B, Aydın, S, Menteşe, E, Bektaş, A. and Dilekçi, G., 2020. Design, synthesis, and characterization of some new benzimidazole derivatives and biological evaluation. *Journal of Heterocyclic Chemistry*, 57(5): 2234-2242.
doi: 10.1002/jhet.3943

Bespalov, A.Ya, Gorchakova, T.L, Ivanov, A.Yu, Kuznetsov, M.A, Kuznetsova, L.M, Pankova, A.S, Prokopenko, L.I. and Avdontceva., M.S., 2015. Alkylation and aminomethylation of 1,3-dihydro-2*H*-benzimidazole-2-thione, *Chemistry of Heterocyclic Compounds*, 50(11): 1547-1558.
doi: 10.1007/s10593-014-1623-z

Champa, R, Vishnumurthy, K, Bodke, Y.D, Bhojya Naik, H, Pushpavathi, I, Meghana, P. and Kadam, P.R., 2023. Synthesis, characterization, and biological investigations of potentially bioactive heterocyclic compounds containing benzimidazole nucleus. *Results in Chemistry*, 6: 101018.
doi: 10.1016/j.rechem.2023.101018

Cheptea, C, Sunel, V, Popovici, C, Dumitrascu, I, Dimitriu, D.G. and Dorohoi, D.O., 2022. Synthesis and quantum mechanical characterization of three new 1-(5-nitro-benzimidazole-2'-yl-sulfonyl-acetyl)- 4-aryl-thiosemicarbazide with biological potential. *Molecular Crystals and Liquid Crystals*, 747(1): 72–80.
doi: 10.1080/15421406.2022.2066794

Coates, J. 2000. Interpretation of Infrared Spectra, A Practical Approach. In: Encyclopedia of Analytical Chemistry, R.A. Meyers (editor), 2000. John Wiley and Sons Ltd, Chichester, pp. 10815–10837.

Desai, N.C, Shah, K.N, Monapara, J, Dave, B.P, Ahmad, I. and Patel, H., 2024. Design, synthesis, biological profiling and molecular modelling studies of heterocyclic benzimidazole analogues as antimicrobial agents. *Journal of Molecular Structure*, 1299: 137166.
doi: 10.1016/j.molstruc.2023.137166

El Ashry, E.S.H, El Kilany, Y, Nahas, N.M, Barakat, A, Al-Qurashi, N, Ghabbour, H.A. and Fun, H.-K., 2016. Synthesis and crystal structures of benzimidazole-2-thione derivatives by alkylation reactions. *Molecules*, 21: 12, 11 pages.
doi: 10.3390/molecules21010012

El-Gohary, N.S. and Shaaban, M.I., 2017. Synthesis and biological evaluation of a new series of benzimidazole derivatives as antimicrobial, antiquorum-sensing and antitumor agents, *European Journal of Medicinal Chemistry*, 131: 255-262.
doi: 10.1016/j.ejmech.2017.03.018

El-Kihel, A, Zouitina, S, Guesmi, S, Ahbala, M, Bauchat, P. and Biersack, B., (2016) Improved Method of S-Alkylation of 2-Mercaptobenzimidazole Derivatives with Trialkylphosphite, *Asian Journal of Chemistry*, 28(6): 1267-1269.
doi: 10.14233/ajchem.2016.19647

Elwakeel, K, Ahmed E, Abdullah A, Mohammed H. and Eric, G., 2021. 2-Mercaptobenzimidazole-functionalized chitosan for enhanced removal of methylene blue: Batch and column studies. *Journal of Environmental Chemical Engineering*, 9(4): 105609, 14 pages.
doi: 10.1016/j.jece.2021.105609

Greenwood, N.N. and Earnshaw, A. 1998(a). Chemistry of the Elements, 2nd Edition, Butterworth-Heinemann, Oxford, 1092 pp.

Greenwood, N.N. and Earnshaw, A. 1998(b). Chemistry of the Elements, 2nd Edition, Butterworth-Heinemann, Oxford, 1132 pp.

Greenwood, N.N. and Earnshaw, A. 1998(c). Chemistry of the Elements, 2nd Edition, Butterworth-Heinemann, Oxford, 1192 pp.

Jakeria, M.R, Toh, R.J, Chen, X.-B. and Cole, I.S., 2022. Evolution and stability of 2-mercaptobenzimidazole inhibitor film upon Al alloy 6061. *Journal of Applied Electrochemistry*, 52: 1021-1044. doi: 10.1007/s10800-022-01687-w

Ji, X, Wang, W, Duan, J, Zhao, X, Wang, L, Wang, Y, Zhou, Z, Li, W. and Hou, B., 2021. Developing wide pH-responsive, self-healing, and anti-corrosion epoxy composite coatings based on encapsulating oleic acid/2-mercaptobenzimidazole corrosion inhibitors in chitosan/poly (vinyl alcohol) core-shell nanofibers. *Progress in Organic Coatings*, 161: 106454. doi: 10.1016/j.porgcoat.2021.106454

Khormali, A. and Ahmadi, S., 2023. Experimental and modeling analysis on the performance of 2-mercaptobenzimidazole corrosion inhibitor in hydrochloric acid solution during acidizing in the petroleum industry. *Journal of Petroleum Exploration and Production Technology*, 13: 2217–2235. doi: 10.1007/s13202-023-01675-6

Lee, J, Park, H.S, Jung, H.J, Park, Y.J, Kang, M.K, Kim, H.J, Yoon, D, Ullah, S, Kang, D, Park, Y, Chun, P, Chung, H.Y. and Moon, H.R., 2023. Anti-browning effect of 2-mercaptobenzo(*d*)imidazole analogs with antioxidant activity on freshly-cut apple slices and their highly potent tyrosinase inhibitory activity. *Antioxidants (Basel)*, 12(10): 1814, 23 pages. doi: 10.3390/antiox12101814

Molou, K.Y.G, Tchambaga, C, Timotou, A, Coulibaly, S, Coulibali, S. and Sissouma, D., 2022. Design, synthesis of bisbenzimidazole dithiol derivatives and analogs, *GSC Advanced Research and Reviews*, 13(02): 085–090. doi: 10.30574/gscarr.2022.13.2.0300

Neshat, C.S, Maurya, I.K, Kumar, V, Tikoo, K, Jain, R. and Kamal, A., 2023. Synthesis, biological evaluation and mechanistic studies of 4-(1,3-thiazol-2-yl)morpholine-benzimidazole hybrids as a new structural class of antimicrobials. *Bioorganic Chemistry*, 136: 106538. doi: 10.1016/j.bioorg.2023.106538

Nuha, D, Evren, A.E, Yılmaz Cankılıç, M. and Yurttaş, L., 2021. Design and synthesis of novel 2,4,5-thiazole derivatives as 6-APA mimics and antimicrobial activity evaluation. *Phosphorus, Sulfur, and Silicon and the Related Elements*, 196(10): 954–960. doi: 10.1080/10426507.2021.1946537

Patle, D, Khurana, N, Gupta, J, Kaur, P. and Khatik, G.L., 2023. Design, Synthesis, and Biological Evaluation of Coixol-based Derivatives as Potential Antidiabetic Agents. *Journal of Molecular Structure*, 1277: 134861. doi: 10.1016/j.molstruc.2022.134861

Popovici, C, Pavel, C.-M, Sunel, V, Cheptea, C, Dimitriu, D.G, Dorohoi, D.O, David, D, Closca, V. and Popa, M., 2021. Optimized Synthesis of New Thiosemicarbazide Derivatives with Tuberculostatic Activity. *International Journal of Molecular Sciences*, 22(22): 12139. doi: 10.3390/ijms222212139

Purwono, B, Nurohmah, B.A, Fathurrohman, P.Z. and Syahri, J., 2021. Some 2-arylbenzimidazole derivatives as antimalarial agents: synthesis, activity assay, molecular docking and pharmacological evaluation. *Rasayan Journal of Chemistry*, 14(1): 94–100. doi: 10.31788/RJC.2021.1416088

Rep, V, Štulić, R, Koštrun, S. *et al.*, 2022. Novel benzimidazoles and benzothiazoles: synthesis, antibacterial activity and ADME profiling. *RSC Medicinal Chemistry*, 13: 1504–1525. doi: 10.1039/D2MD00143H

Rizvi, S.F.A, Zhang, H, Mehmood, S. and Sanad, M., 2020. Synthesis of $^{99m}$Tc-labeled 2-mercaptobenzimidazole as a novel radiotracer to diagnose tumor hypoxia. *Translational oncology*, 13(12): 100854. doi: 10.1016/j.tranon.2020.100854

Rodríguez, O.A.R, Sánchez, J.P.M, Gamiño, J.A.V, Benicio, F.O, Hernández, C.E.M, Martínez, M.T.S, Martínez, F.J.M, Sandoval, Z.G. and Ramos-Organillo, Á., 2021. Synthesis of novel amides with antiradical capacity from 2-mercaptobenzimidazole and cinnamic acids: Evaluation through donor-acceptor maps and QSAR. *Journal of Molecular Structure*, 1223: 128917. doi: 10.1016/j.molstruc.2020.128917

Sarıkaya, G, Çoban, G, Parlar, S, Tarikogullari, A.H, Armagan, G, Erdoğan, M.A, Alptüzün, V. and Alpan, A.S., 2018. Multifunctional cholinesterase inhibitors for Alzheimer's disease: Synthesis, biological evaluations, and docking studies of o/p-propoxyphenylsubstituted-1H-benzimidazole derivatives. *Archiv der Pharmazie*, 351(8): 1800076, 18 pages. doi: 10.1002/ardp.201800076

Singh, W.M. and Baruah, J.B., 2008. Rosolic Acid–Catalyzed Conversion of Thiols to Disulfides. *Synthetic Communications*, 39(2): 325-331. doi: 10.1080/00397910802372590

Subimol, K.R, Arul Antony, S. and Karthik Kumar, K., 2015. A novel and facile methodology for synthesis of coumarin coupled benzimidazole-*2-thione compounds. Phosphorus, Sulfur, and Silicon and the Related Elements*, 190(4): 494-502. doi: 10.1080/10426507.2014.952000

Theodore, C.E, Sivaiah, G, Benaka Prasad, S.B, Yogesh Kumar, K, Raghu, M.S, Alharethy, F, Prashanth, M.K. and Jeon, B.-H., 2023. Design, synthesis, anticancer activity and molecular docking of novel 1H-benzo[d]imidazole derivatives as potential EGFR inhibitors. *Journal of Molecular Structure*, 1294 (Part 2): 136341. doi: 10.1016/j.molstruc.2023.136341.

Wei, X, Zhong, M, Wang, S, Li, L, Song, Z.L, Zhang, J, Xu, J. and Fang, J., 2021. Synthesis and biological evaluation of disulfides as anticancer agents with thioredoxin inhibition. *Bioorganic chemistry*, 110: 104814, 14 pages. doi: 10.1016/j.bioorg.2021.104814

Zhang, T, Wang, R, Ma, L, Liu, J, Sun, J. and Wang B., 2022. High-efficiency synthesis of sulfenamides and disulfides by electrochemical dehydrogenative coupling. *Environmental Chemistry Letters*, 20: 2765–2771. doi: 10.1007/s10311-022-01459-0